Title
FIELD ION INVESTIGATIONS OF Ta-Mo SOLID SOLUTIONS

Authors
Raghavan, N. Durai
Ranganathan, S.
Thomas, G.

Publication Date
1967-12-01

UCRL-17711 Rev.

Cy. 2

University of California

Ernest O. Lawrence Radiation Laboratory

FIELD ION INVESTIGATIONS OF Ta-Mo SOLID SOLUTIONS

N. Durai Raghavan, S. Ranganathan, and G. Thomas

December 1967

DISCLAIMER

Submitted to Acta Met.

UCRL-17711-Rev.
Preprint

UNIVERSITY OF CALIFORNIA

Lawrence Radiation Laboratory
Berkeley, California

AEC Contract No. W-7405-eng-48

FIELD ION INVESTIGATIONS OF Ta-Mo SOLID SOLUTIONS

N. Durai Raghavan, S. Ranganathan, and G. Thomas

December 1967

FIELD ION INVESTIGATIONS OF Ta-Mo SOLID SOLUTIONS

N. Durai Raghavan,[†] S. Ranganathan,[††] and G. Thomas[§]

Inorganic Materials Research Division, Lawrence Radiation Laboratory,
Department of Mineral Technology, College of Engineering,
University of California, Berkeley, California

December 1967

ABSTRACT

A field ion microscope study of the tantalum-molybdenum system has been carried out at liquid hydrogen temperatures. The purpose of this investigation was twofold; the first being to increase the knowledge on the field ion microscopy of alloys, and the second being to categorize the segregation effects that become important at the high concentration levels to make the alloys brittle. Micrographs have been obtained from three alloys of the composition Mo-8 Ta, Mo-50 Ta and Ta-10 Mo and from the two pure metals. The Ta-Mo alloy micrographs obtained show far more irregularity than those from W-Mo alloys. The greater regularity of the Mo-8 Ta micrographs over those from Ta-10 Mo has been shown to be in accord with predictions based on field evaporation from dilute alloys and the unexpected large difference in the regularity has been accounted for by considering the polarization and heat of solution terms in the field evaporation equation.

---

§ Inorganic Materials Research Division, Lawrence Radiation Laboratory, and the Department of Mineral Technology, College of Engineering, University of California, Berkeley, California.

† Now of: The Franklin Institute, Research Laboratories, Philadelphia, Pennsylvania 19103.

†† Now at: Banaras Hindu University, Varanasi-5, India.

Computer simulation of images from random and clustered alloys has been performed on the assumption that solute atoms do not participate in image formation. The far too great regularity of such computed images indicates that the total invisibility criterion is an oversimplification. A band structure results when deviations from randomness become appreciable in the clustered alloy. Contrast to be expected from a demixed alloy in the Ta-Mo system has been discussed, but the available experimental evidence did not reveal such contrast effects. It has been concluded that the width of such demixed zones probably exceeds 1000Å. However, a tendency for local clustering on the [200] planes was observed in the Ta-50 Mo alloy.

1. INTRODUCTION

The field ion microscope is capable of a resolution of 2-3Å and therefore can display the atomic arrangement on a metal surface. The microscope is thus ideally suited for investigations in which the behavior of atoms in a metal crystal is to be considered. In particular it has shed valuable information in the study of lattice imperfections, structure of metals and alloys, and the dynamics of radiation damage. Such information has been mostly obtained from pure metals, the micrographs of which are characterized by extreme regularity. The field ion microscope study of alloys, however, has progressed at a much slower pace. Except in the case of ordered alloys, the ion images from alloys are extremely irregular. A significant limitation imposed by such a lack of crystallographic regularity is that it is very difficult to recognize and determine the nature of any lattice defects present.

In the past, two systems, namely the W-Mo system and the W-end of the W-Re system, have been studied quite extensively. Caspary and Krautz[1] who investigated the W-Mo system, obtained micrographs from alloys containing 25, 50 and 75% Mo, and compared them with those of pure W and Mo. They found that the irregularity in the images increased towards the Mo-end. They concluded that the random surfaces are due to preferential evaporation of Mo. Ralph and Brandon[2] who studied the W-end of the W-Re system, looked at two single phase alloys, viz., W-5 a/o Re and W-26 a/o Re and a two-phase alloy containing 34% Re. The single phase concentrated alloy was found to yield very irregular images. The two-phase alloy was shown to exhibit contrast due to the σ-phase. They also presented evidence to suggest that Re atoms tend to cluster and advanced a method to

distinguish between the atomic species. Work on individual alloys has been conducted to understand specific phenomena such as field evaporation. DeBroff and Machlin[3] studied the field evaporation and imaging characteristics of dilute solid solutions of gold, cobalt, nickel, tungsten, and palladium in platinum. They interpreted the vacancies observed on high index planes to arise out of preferential evaporation of solute atoms or of solvent atoms or of both.

It is therefore evident that a deeper understanding of how the solute modifies the field ionization and the evaporation characteristics of the solvent is possible only with more data on alloys. In choosing a system, attention was directed towards the four metals of Groups VB and VIB, viz., Nb, Ta, Mo and W. In addition to their refractoriness, these alloy systems possess interesting mechanical properties. Of the six possible binary alloy systems of these four metals only Nb-Ta and Mo-W are ductile at all alloy compositions. The rest show cleavage behavior at high alloy concentrations.[4,5] As mentioned before, the W-Mo system, belonging to the ductile group, has been studied extensively. Considerable information on the Ta-Mo system belonging to the other group is available. Tantalum and molybdenum form completely miscible solid solutions with each other as do all the other binary alloys of the four refractory metals, Nb, Ta, Mo and W. Previous work on the Ta-Mo system[6] has shown that alloys in the composition range of Mo-19 Ta to Mo-58 Ta cleave on the {100} planes. X-ray intensity measurements indicated that there exist deviations from random solid solution in these alloys and it was suggested that cleavage occurs due to a violation of the strain energy restrictions on the elastic coefficients in a local region of the crystal. It was therefore decided

to study the Ta-Mo system since the investigation, besides providing useful information on alloys, can be expected to throw light on the nature of this demixing.

2. EXPERIMENTAL PROCEDURES

2.1 Low Temperature Microscopy

The present study was conducted in a stainless steel microscope fitted with a liquid hydrogen cryotip.[7] In the cryotip, which is an open-cycle Joule-Thomson refrigerator, a small volume (2-5 cc) of liquid hydrogen is generated and maintained in a sealed portion of the microscope, thereby eliminating hazards due to storage, handling and transfer.

2.2 Specimen Preparation

Tantalum and molybdenum are available in the form of 10 mil wires and can therefore be directly used for preparing field ion specimens. In the case of the alloys, the alloy crystals were first obtained as rods grown in an electron beam zone refiner, by melting together proper combinations of tantalum and molybdenum rods of different diameters. The homogeneity of the alloys was checked with an electron microprobe analyzer. The composition deviations over 100μ intervals were found to be less than 3%. The exact compositions of the alloy crystals were then determined by lattice parameter measurements and by comparing the observed lattice parameter with previous lattice parameter data on the Ta-Mo alloy system.[6] The compositions of the alloys grown were determined to be Ta-10 a/o Mo, Mo-8 a/o Ta, and Ta-47 a/o Mo. The Ta-47 a/o Mo alloy, for convenience, will from now on be referred to as the Ta-50 Mo alloy. The two end alloys were

successfully reduced to wire form by a combination of swaging and cold rolling. This method was found not to be applicable for the Ta-50 Mo alloy, which is too brittle. Spark cutting has proved to be the only method that is fairly successful. Twenty mil thick wires were found to be of the optimum dimension. Thinner wires crumbled while spot welding to the nickel wire of the specimen holder preparatory to electropolishing, whereas thicker wires took too long for polishing. Fine tips suitable for field ion microscopy were obtained from these wires by electropolishing. Mo and Mo-8 a/o Ta alloys are both conveniently polished in a 20% aqueous solution of KCN at 5-10 volts ac, employing the double layer method. The polishing of Ta-10 a/o Mo and Ta-50 a/o Mo is considerably more difficult. These wires were electropolished in an electrolyte consisting of 4 parts of HF, 2 parts of H_2SO_4, 2 parts of H_3PO_4, and 1 part of acetic acid to which some HNO_3 was added. An iridium cathode was used and polishing was done at 10-15 volts dc, 0.1-0.15 amps, and -10 to -20°C. The low temperature was meant to reduce oxygen and hydrogen pickup. The method is not reproducible; in particular Ta-10 a/o Mo specimens gave extra difficulty while polishing. The tips were either blunt or swiftly destroyed by flashing in the microscope, apparently due to oxygen embrittlement during polishing.

3. RESULTS

3.1 Pure Tantalum

Figure 1 is a helium ion micrograph of pure Ta obtained at 21°K. The field evaporation and form of Ta have been discussed by Nakamura and Müller[8] in detail. Tantalum is observed to develop a large number of planes, in particular {200} (which is developed poorly in W and Mo), with excellent

resolution. The micrograph has characteristic intensity distribution; the square {002} region bounded by {011} planes is bright, whereas the triangular {222} region also bounded by {011} planes is dim except for the {222} planes themselves. The region extending from the {112} to {114} is found to be characterized by a random appearance brought about by a rearrangement of atoms. The prominent spots in these regions have been suggested[8] to be due to metal atoms in a low coordination site.

3.2 Molybdenum

Figure 2 is a field ion micrograph of Mo at 21°K. The number of planes appearing well developed and well resolved is considerably less than in Ta. This is to be attributed to the higher strength of the Ta lattice, as well as the poor working range of Mo. In Mo the {222} regions, in particular, yield under the shear component of the field stress. Müller[9] has suggested that the dislocation loops formed as a result of this yielding are responsible for the random appearance of the {222} planes in Mo. The dislocation loop contrast obtained in field-ion micrographs has been considered carefully by Durai Raghavan, Petroff, and Ranganathan.[10] The intersection of a loop on the specimen surface results in well-defined image contrast due to the two line segments, the nature of which is defined by the Burgers vector and the habit plane of the loop. It is to be concluded that the presence of dislocation loops cannot be the primary cause for this random appearance of {222} planes in Mo. The Mo micrographs show other differences, as well, from the Ta patterns. The intense square region of {100} in Ta is dim in Mo while the weak regions around {111} in Ta are exceedingly bright. The presence of low coordination sites identified

by their brightness is not observed. The [001] zone decoration line running between {011} and {002} planes, totally absent in Ta, is observed, though not in as clear a fashion as in W.

3.3 Mo-8 Ta Alloy

Of the alloys of the Ta-Mo system studied, Mo-8 Ta gave the most regular images. Figure 3 is a typical field ion micrograph from a Mo-8 Ta tip. The orientation is an unusual <100> compared to the normal <110> texture developed by Ta, Mo, and W. This is obviously due to the severe deformation introduced during the reduction of the alloy rod to a wire and the subsequent annealing. All the specimens of this alloy, that were looked at in the microscope, exhibited the same orientation.

The intensity difference on either side of the {112} planes is found to be much less marked than in the micrographs of Mo-8 Ta imaged at 77°K. A similar feature has been observed in Ta micrographs.[8] A good number of planes like {110}, {112}, {310}, and {222} are all observed to be well developed. The {222} region of Mo which generally appears with poor resolution is delineated with much better resolution in these micrographs. A long series of pictures from this alloy tip was taken using a pulse generator with single pulses of height 1 kV and a width of 30 μsec. All the Mo-8 Ta micrographs, obtained in such an evaporation sequence, show a small number of bright spots in the usually less intense region between (110) and (200) planes and a small number of weak spots in the intense triangular region. The Ta atoms, on the other hand, are expected to be bright in the first region and weak in the second. This leads to the possibility that there could be a one-to-one correspondence between such

spots and Ta atoms. Thus Figs. 4a and 4b, which were obtained in consecutive field evaporation pulses, show the evaporation of a group of atoms tentatively identified as Ta atoms.

3.4 Ta-10 Mo Alloy

Figure 5 shows a helium ion micrograph from a Ta-10 Mo tip. The addition of 10 a/o of molybdenum is seen to have disturbed the field ion image extensively. Since the addition of Mo also results in considerable strengthening of Ta, the appearance of such random surfaces cannot be due to lattice deformation by the field stress. The good resolution in the {110} and {130} regions rules out the possibility that the specimen did not quite attain low temperatures.

The addition of Mo also results in a good number of dark regions where no imaging is apparently taking place, and which persists during field evaporation (Fig. 6). This is perhaps due to preferential field evaporation of one species. Significantly present are also a large number of bright spots which are also not removed by extensive field evaporation.

3.5 Ta-50 Mo Alloy

Figure 7 shows the helium ion micrograph of a Ta-50 Mo tip. The micrograph is characteristic of a concentrated alloy in that only a few planes, e.g., (110), (112), (222) and (310) are adequately resolved. The image is observed to be lacking in the characteristics of pure Ta or Mo and in fact is more similar to that from W alloys. The image intensity is uniform throughout the entire micrograph. This is to be expected, however, since the composition corresponds to that of the middle alloy and

Ta and Mo are complementary in their image intensity relationship.

The number of spots also appears to be significantly less than would be expected from a tip of 300Å radius. Furthermore, almost all of the spots appear to be bright. These observations suggest that perhaps not all the surface atoms are participating in image formation, and those that are giving rise to image spots are perhaps in protruded positions on the surface.

Figures 8a-c are a sequence of micrographs from a Ta-50 specimen showing the effect of local clustering. The (200) plane in Fig. 8a is found to be well developed. Figure 8b was obtained by field evaporation of the surface of Fig. 8a with a small pulse and it is seen that the (200) region has become less regular. After the removal of seven more atom planes Fig. 8c was obtained. The micrograph now shows the appearance of a more regular (200) region. This series, and others done in the same way, indicate that the composition is fluctuating and could be explained by clustering over regions of 25Å in diameter.

4. DISCUSSION

4.1 General Features

Since Caspary and Krautz[1] have previously performed a similar study on the W-Mo system, it is interesting to compare the micrographs obtained from the two systems. When this is done, it is obvious that the ion images from the Ta-Mo system are considerably more irregular. Table 1, which compares the planes that are identifiably present in the Mo alloy series, well substantiates this point. The increased irregularity in the Ta-Mo images assumes greater significance since the two end alloys of the Ta-Mo

Table 1. List of planes appearing in field ion images of Ta-Mo alloys and W-Mo alloys[2]

Zones uvw	Planes		Mo Content (a/o) of the Ta-Mo Alloys					Mo Content (a/o) of the W-Mo Alloy				
	hkℓ	$h^2+k^2+\ell^2$	0	10	50	92	100	0	25	50	75	100
[100]	110	2	x	x	x	x	x	x	x	x	x	x
	200	4	x	x	x	x	x	x	x	x	x	x
	310	10	x	x	x	x	x	x	x	x		x
	510	26	x				x	x				
	530	34	x					x				
	640	52										
[111]	110	2	x	x	x	x	x	x	x	x	x	x
	211	6	x	x	x	x	x	x	x	x	x	x
	321	14	x			x	x	x	x	x		x
	431	26	x				x	x	x			x
	541	42	x					x				
[110]	110	2	x	x	x	x	x	x	x	x	x	x
	200	4	x	x	x	x	x	x	x	x	x	x
	211	6	x	x	x	x	x	x	x	x	x	x
	222	12	x	x	x	x	x	x	x	x	x	x
	411	18	x			x	x	x	x	x	x	x
	332	22	x					x	x	x	x	x
	433	34	x					x	x	x		x
	442	36	x					x	x			x
	611	38						x	x			
	622	44						x				
	552	54						x				
	644	68						x				
	662	76						x				

UCRL-17711-Rev.

system studied are quite dilute compared to the two of the W-Mo system studied by Caspary and Krautz. An asymmetry similar to the one observed about the 50% solute in the W-Mo system can be observed to be present in the Ta-Mo micrográphs as well, but the sense of this asymmetry is opposite. In W-Mo, the W-based alloys are more regular over a larger solute concentration, whereas in the Ta-Mo system it is the Mo-based alloy that is found to be more regular. It should, however, be noted that the compositions of the alloys of the two systems studied are not the same.

4.2 Field Evaporation in Ta-Mo Alloys

Field evaporation is now well recognized to affect the nature of alloy micrographs mainly through the preferential evaporation or retention of the solute in the lattice. This approach has been recently employed by Brandon[11] in the case of field evaporation from dilute alloys. A similar viewpoint has been taken in the discussion below towards understanding the field evaporation process.

The activation energy Q'_B necessary to field evaporate a B atom from the surface of a dilute alloy of B in A can be calculated by considering the following cycle:

1. Evaporate a B atom.
2. Ionize it n times where ne is the charge with which B is ionized in the field evaporation process.
3. Return the n electrons to the matrix A.

Q'_B is therefore given by:

$$Q'_B = \lambda_B + \Sigma I_n^B - n\phi_A + P(B)$$

where λ_B is the sublimation energy of B in A, I_n^B is the nth ionization potential of B, ϕ_A is the work function of A and P(B) is the polarization correction appropriate to the B atom. λ_B is given by $\lambda_o^B + H_S$ where λ_o^B is the sublimation energy of pure B and H_S is the heat of solution.

Since the alloy is dilute, the activation energy Q_A' for evaporation of A can be equated to its activation energy Q_A^o of pure A. Q_A' is thus given by:

$$Q_A' = Q_A^o = \lambda_A + I_n^A - n\phi_A + P(A),$$

where the parameters have the same meaning as before, but refer to the species A. For convenience, it has been assumed here that both A and B ionize with the same charge ne in the field evaporation process.

Since the difference in the two activation energy values will decide which component will be preferentially field evaporating and to what extent, we determine $Q_A' - Q_B'$ to be:

$$Q_A' - Q_B' = H_S + (\lambda_A - \lambda_B) + (\Sigma I_n^A - \Sigma I_n^B) + P(A) - P(B)$$

This expression is exact for field evaporation of A and B from the same or equivalent sites in the lattice. For atoms on different sites (sites that are on different planes or that have different coordination, etc.) the differences in binding energy and in the field enhancement factors operating at the two sites must be taken into consideration.

Brandon[11] has discussed in detail the case where the solute atoms, represented by B in our discussion, are preferentially evaporated and has

predicted that the field ion images from a dilute alloy of a refractory metal in a less refractory matrix will be more regular than the image from the alloy of some components, but with atomic fractions reversed. This is indeed observed to be the situation with respect to the end alloys of the Ta-Mo system. However, to explain the unexpected large differences in the regularity of these micrographs, we have to consider the factors affecting field evaporation. These are:

1. $\Delta\lambda$, the differences in sublimation energies of A and B;
2. ΔI, the differences in the ionization potentials of A and B;
3. polarization differences, P(A) - P(B); and
4. heat of solution.

Except for $\Delta\lambda$, all the other terms are only poorly known for the refractory metals, which are commonly studied with the field ion microscope. Still, many useful qualitative conclusions can be drawn by considering them carefully. Since the calculated evaporation fields of pure metals do not include polarization corrections, the first two factors can be conveniently treated together and their effect will be indicated by the differences in the calculated evaporation fields Q_A and Q_B for these metals, provided their work functions are not very different as in the case with Ta, Mo and W. These are listed in Table 2. Polarization differences have to be determined in an empirical manner. Of the three refractory metals, W, Mo, and Ta, Mo does not show the presence of atoms occupying low coordination sites. In W, such atoms are observed, which are removed by field evaporation at 77°K. In Ta, on the other hand, they persist till field evaporation at 300°K. It has already been mentioned that such low coordination

Table 2. Some useful properties of Mo, Ta and W

Z	Element	ϕ (eV)	Λ (eV)	Q° (v/A)	$\Delta\gamma \cdot \gamma_a^2$ $\AA^3$	χ $cm^2/Kg \times 10^6$
42	Mo	4.30	6.15	3.8	0.74	0.36
73	Ta	6.15	8.25	4.6	0.96	0.48
74	W	4.52	8.67	5.7	0.77	0.31

ϕ work function

Λ sublimation energy

Q° evaporation field for evaporation as a doubly charged ion

χ compressibility

sites are stabilized by field penetration polarization and it can, therefore, be concluded that the polarization effects are strong in Ta but much less so in Mo and W. This conclusion is supported by a comparison of the compressibility, χ, which can be used as an index for the magnitude of the polarization effect.[12] Thus a large value of χ indicates a large P. From Table 2, which lists the properties of Ta, Mo and W, it is seen that Ta has the largest compressibility. In accordance with this criterion, Nb, which has an even higher χ than Ta, should also show a strong tendency for stabilization of low coordination sites and indeed Nb micrographs show such occurrence of a large number of spots occupying metastable sites.[13]

The heats of solution, also, have to be similarly determined since thermodynamic data for these systems do not exist. According to quasi-chemical theory, the heat of solution is positive if clustering occurs and negative if ordering is favored. In the Ta-Mo system, it has been shown[6] that there is a clustering situation in the Ta-end of the Ta-Mo phase diagram and thus a positive heat of solution is inferred. The polarization effects of Ta and Mo have already been discussed and it was shown that P(Ta) - P(Mo) is expected to be large and positive. Since, as Müller[12] has shown in the case of W, the polarization term will get larger for the high index planes, ΔP for Ta-Mo alloys would also increase for such planes. These two positive contributions along with the positive ΔQ ($= Q'_{Ta} - Q_{Mo}$; see Table 2) will therefore make $Q'_{Ta} - Q'_{Mo}$ quite large. For this reason, it appears that the Ta-Mo micrographs are exceedingly disorganized in spite of the low solute content. It is also easy to see why this effect is not too pronounced in the W-Mo system. The compressibility data indicate that the polarization corrections should be approximately equal for W and Mo and

from the absence of any clustering, the heat of solution is inferred to be zero or negative. Thus $Q'_{Ta} - Q'_{Mo}$ is not large enough to cause serious irregularity in the W-Mo micrographs.

For any alloy system, Brandon's rule[11] for the case of dilute alloys can be expected to hold true. The difference in the regularity of the two end alloys will be controlled by the difference $Q'_A - Q'_B$ and as seen above, this difference will be modified by both the polarization corrections and the deviation from randomness. Of the four refractory metals Nb, Ta, Mo, and W, as shown in the section on polarization, Nb and Ta have high polarization corrections. If we associate short range ordering with a negative heat of solution and clustering with a positive heat of solution -- this is true for dilute alloys -- for the Nb-Mo, Nb-W, Ta-Mo and Ta-W systems, the application of Vegard's law to the Nb and Ta ends indicates clustering and therefore a positive heat of solution. Since the polarization corrections also for the system will be large and positive, these alloys also will give irregular images at the Nb and Ta ends. Mo-W and Nb-Ta, on the other hand, are expected to yield fairly regular images at both ends.

4.3 Computer Simulation

In general, the alloy micrographs do not develop high index planes, show the presence of dark or pitted regions where no imaging is probably taking place and a large number of bright spots which have been shown to be attributed to the field ionization and evaporation processes in the alloy and as we have already observed, these processes are modified to a considerable extent by the presence of the solute.

For understanding the contrast from alloys, it is, therefore, helpful

to consider the effect of the field ionization and the field evaporation processes together as a single parameter. In order to check whether a single visibility criterion unifying the field ionization and evaporation processes can lead to random surfaces characteristic of the alloy micrographs, a computer program has been performed. It is now well realized that the general features of the field ion image of a pure metal can be explained in terms of the geometry of the approximately spherical surface which is obtained when a crystal lattice is cut by a sphere. Moore[13] was the first to point out that by assuming that only those atoms that lie within a shell of given thickness can give rise to spots, image patterns that strongly resemble the field ion images can be obtained with the help of a computer. Recently Moore[13] has extended this work to solid solution alloys. To account for the different evaporative properties of the two species, he assigned different shell thicknesses. A similar program, but based on a different criterion described below, has been performed on alloys of different compositions.

Since the field ion images of the BCC metals Mo, Nb, W, and Ta generally correspond to a <110> wire texture, it was decided to obtain computed images corresponding to a <110> orientation. For this purpose the program developed by Ranganathan et al.[14] was suitably modified. The coordinate axes are chosen to be [110], [1$\bar{1}$0] and [001]. With this set of axes, the BCC lattice becomes a face centered tetragonal one with a c/a ratio of 0.703 (= $1/\sqrt{2}$). It is therefore necessary to consider four primitive tetragonal lattices with origins at 0 0 0; $\frac{1}{2}\,\frac{1}{2}$ 0; $\frac{1}{2}$ 0 $\frac{1}{2}$; and 0 $\frac{1}{2}\,\frac{1}{2}$. Since the stereographic projection is a nearer approximation to the field ion image, the orthographic coordinates were first converted to the stereographic

ones and the Cal-Comp plotter subroutine was used to plot the simulated image. The computations were programmed in FORTRAN for Control Data 6600 Computer. Figure 9a gives the computed image for a BCC metal of radius 200a where a is the lattice parameter.

4.3.1 Random Alloys

The above program corresponds to the case of a pure metal. First the random alloys were considered. For the application of the visibility criterion, according to which the solute atoms are totally invisible, a control statement was introduced that permitted the coordinate of an atom to be recorded only if the random number generation function exceeded the solvent content of the alloy. This allows for a random distribution of the two species with the solute atoms not participating in the image.

Figures 9b and 9c show the computed images for BCC lattice with compositions of 90% and 50% of solvent. The computed images correspond to a radius of 200a and the value of p, the shell thickness, was chosen to be 0.05a. The computed images from the 50% solvent alloy are somewhat irregular. A comparison of these images with those obtained from the Ta-Mo system or the W-Mo system clearly indicates the field ion patterns from alloys are considerably more irregular than the computed images. A count of the spots from the micrographs of the Ta-Mo alloys with 10% and 50% solute contents does not indicate a sharp reduction in the number of spots as is the case with the computed images. Further, since it is only the appearance of a few rows of atoms in any plane that makes the plane recognizable, it follows that the onset of irregularity is a critical function of the radius and that for the same

alloy there will be improvement in regularity with increase in radius. Prolonged field evaporation of the Ta-Mo alloys resulting in considerable change of the radius was observed not to have any marked improvement of the regularity of ion images. A similar observation has been made by Brenner[7] on the regularity of Pt-10 Ir alloy micrographs during prolonged field evaporation. It is to be concluded that the total invisibility criterion is too great an oversimplification to yield computed images comparable to the observed alloy micrographs.

4.3.2 Clustered Alloys

So far, a random distribution has been assumed for the atomic species of the alloy. When deviations from such randomness exist, the contrast to be expected will be, in general, partly due to the intrinsic imaging behavior of the species, modified by the presence of the second component, and partly due to the interface effect. An interface can be defined to separate regions of a crystal different in structure and/or composition. While the interface effect is, therefore, not important for a random distribution or short range ordering, it should have marked influence in the case of clustering, since a clustered situation necessarily implies regions of different composition. The interface effect, however, will be confined to the interface only.

To understand the type of contrast that can be expected from clustered alloys, computations were performed with a specific model of clustering. A model, whereby the composition varied in a sinusoidal manner radially along the crystal, was assumed in order to minimize computational difficulties. The radial distribution ensured that there is no crystallographic habit for

the clustering present.

For this clustering case, the parameters that can be varied are the period and amplitude of the sinusoidal variations of the composition. The mean composition was held at 50-50 and the clustering period was assumed to be fifteen (110) planes (= 15 $a/\sqrt{2}$ Å where a is the lattice parameter). To introduce this clustering model, the distance of an atom that lay within any annulus from the apex was calculated and converted into $2R\Pi + \theta$ radians by dividing by 2Π/period. Then $\alpha \cos \theta + 0.5$, where α is the clustering amplitude, is the solvent concentration on the spherical surface with radius corresponding to the distance of the atom under consideration from the apex (Fig. 9d). Now the visibility consideration is applied by the control statement that allows the recording of the atom coordinates only if the random generating function exceeded $\alpha \cos \theta + 0.5$. This was repeated for all atoms in any annulus.

Figures 9e and 9f show the computed images from a 50-50 alloy with a clustering distribution. The period is a constant $15a/\sqrt{2}$Å for both cases and the amplitudes are 0.1 and 0.4, respectively. It is seen that the computed image for the case of small deviations is as irregular as those from random alloys of the same composition. When the deviation has increased to 0.4 a band structure is developed. The regions with fewer spots, obviously, correspond to the regions where solute atoms are concentrated. Though the weakness of the total invisibility criterion becomes again readily apparent, the interface effect offers some insight as to the nature of micrographs obtainable from clustered alloys. It is seen that the band structure becomes marked only if the deviations from the random composition are substantial and also if the width of the clustered zone is small in

comparison to the radius of the tip. When clustered regions have a larger width, it is clear that the interface effect can be missed.

4.3.3 Demixed Alloys

A case where clustering width exceeds such limits is that of a demixed alloy. In this situation, it is not possible to detect the demixing effects from a single micrograph. The interesting case of demixing reported in Ta-Mo alloys in the high concentration range[6] has already been mentioned. Segregation of the two species here occurs with a crystallographic habit. In the Mo-rich alloys this composition deviation is on a {200} plane and in the Ta-rich alloys the deviations occur on {110} planes. The result of such demixing is the formation of domains richer in either of the two components of the alloy than warranted by the nominal composition. It is well known that though Ta and Mo are BCC metals of the transition type their ion images display distinct singularities. Each has an image of typical but different intensity distribution. Also Ta develops {200} planes very well while Mo does not. Thus on crossing from a Ta-rich region to a Mo-rich region the image characteristics should change in a marked fashion. Experimentally, pulsed field evaporation was performed on a number of Ta-50 Mo tips. About 200 micrographs covering a distance of about 800Å were obtained in a single field evaporation sequence and were analyzed for effects mentioned above. Except for local clustering effects, evidence for demixing was not detected. This could very well mean that the width of demixed zones is larger than 1000Å.

5. CONCLUSIONS

A field ion microscope study of the tantalum-molybdenum system has

been carried out at liquid hydrogen temperature. The Ta-Mo alloy micrographs obtained are far more irregular than those from W-Mo alloys. The greater regularity of the Mo-8 Ta micrographs over those from Ta-10 Mo alloy has been found to be in accord with predictions based on field evaporation from dilute alloys and an attempt has been made to explain the rather large difference in their regularity by considering the polarization and the heat of solution terms in the field evaporation equation. The far too regular computed images from random alloys obtained on the assumption that solute atoms do not participate in imaging indicate that a total invisibility criterion is an over-simplification. In the case of clustered alloys a band structure has been found to result when the deviation from randomness is appreciable. Pulsed field evaporation on the Ta-40 Mo alloy has provided evidence for local clustering, but did not reveal any contrast effects to be expected from a demixed state. It has been concluded that the width of the demixed zones exceeds 1000Å.

ACKNOWLEDGMENTS

This research was done under the auspices of the United States Atomic Energy Commission, through the Inorganic Materials Research Division of the Lawrence Radiation Laboratory. This research was performed in partial fulfillment of the Ph.D. degree at the University of California, Berkeley (N. D. R.).

REFERENCES

1. E. K. CASPARY and E. KRAUTZ, Z. Naturforsch. 19a, 591 (1964).

2. B. RALPH and D. G. BRANDON, Phil. Mag. 8, 919 (1963).

3. W. DeBROFF and E. S. MACHLIN, Proceedings of the 13th Field Emission Symposium, Cornell University, New York, 1966.

4. R. KIEFFER, K. SEDALATCHEK and H. BRAUN, J. Less Common Metals 1, 19 (1959).

5. H. R. SMITH, et al., Niobium, Tantalum, Molybdenum and Tungsten, Sheffield Conference 1960, edited by A. G. QUARRELL. Elsevier Publishing Company, Amsterdam (1961).

6. L. I. VAN TORNE and G. THOMAS, Acta Met. 14, 621 (1966).

7. S. S. BRENNER, High-Temperature, High-Resolution Metallography, Proceedings of a Symposium sponsored by the Ferrous Metallurgy Committee, Institute of Metals Division, The Metallurgical Society, AIME, Chicago, Illinois, February 15, 1965, p. 281. Gordon and Breach Science Publishers, New York, N. Y. (1967).

8. S. NAKAMURA and E. W. MÜLLER, J. Appl. Phys. 36, 2535 (1965).

9. E. W. MÜLLER, J. Phys. Soc. Japan 18, Suppl. II (1963).

10. Unpublished.

11. D. G. BRANDON, Surface Science 3, 1 (1965).

12. E. W. MÜLLER, Surface Science 2, 484 (1964).

13. A. J. W. MOORE, Phil. Mag. (in press).

14. S. RANGANATHAN, H. R. LYON and G. THOMAS, J. Appl. Phys. (in press).

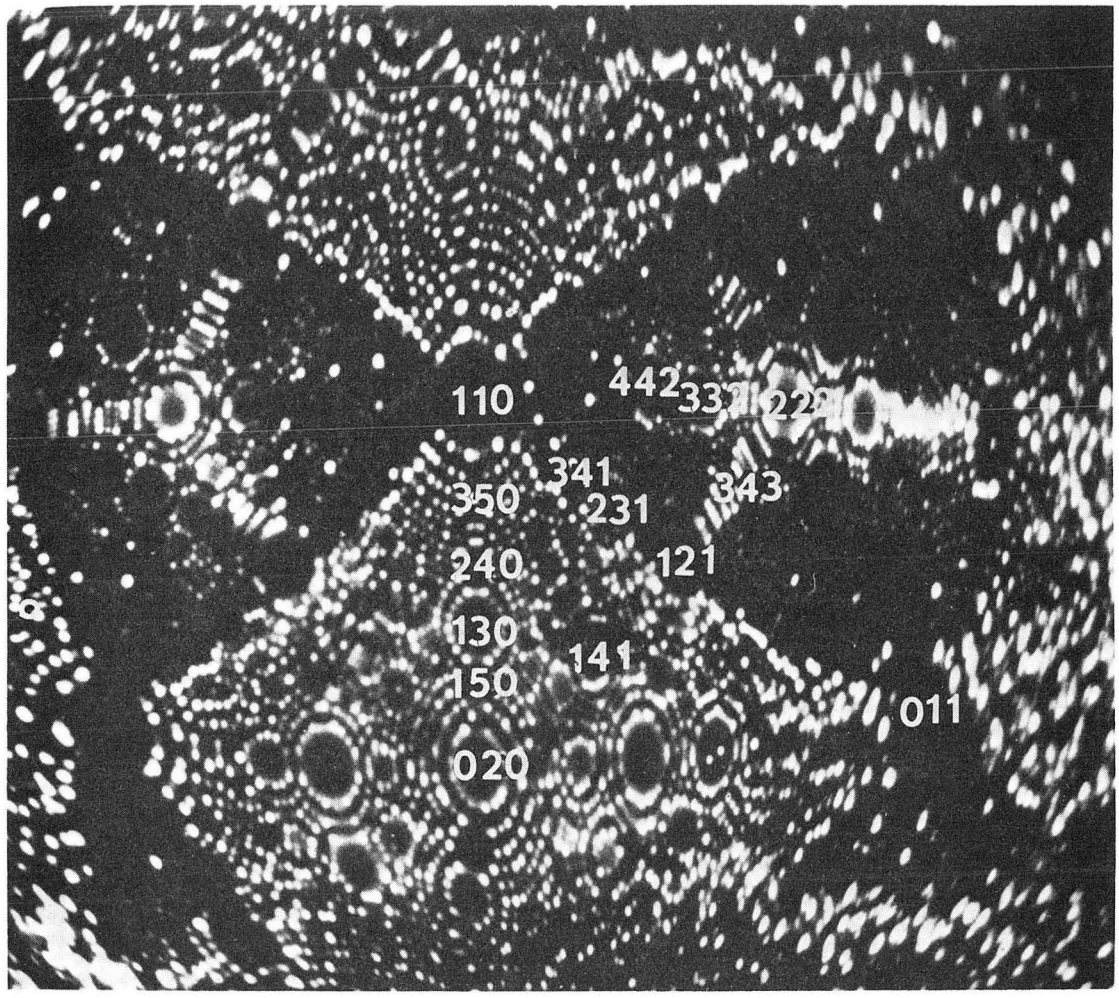

XBB 678-4452

Fig. 1 Helium ion micrograph of Ta at 21°K.

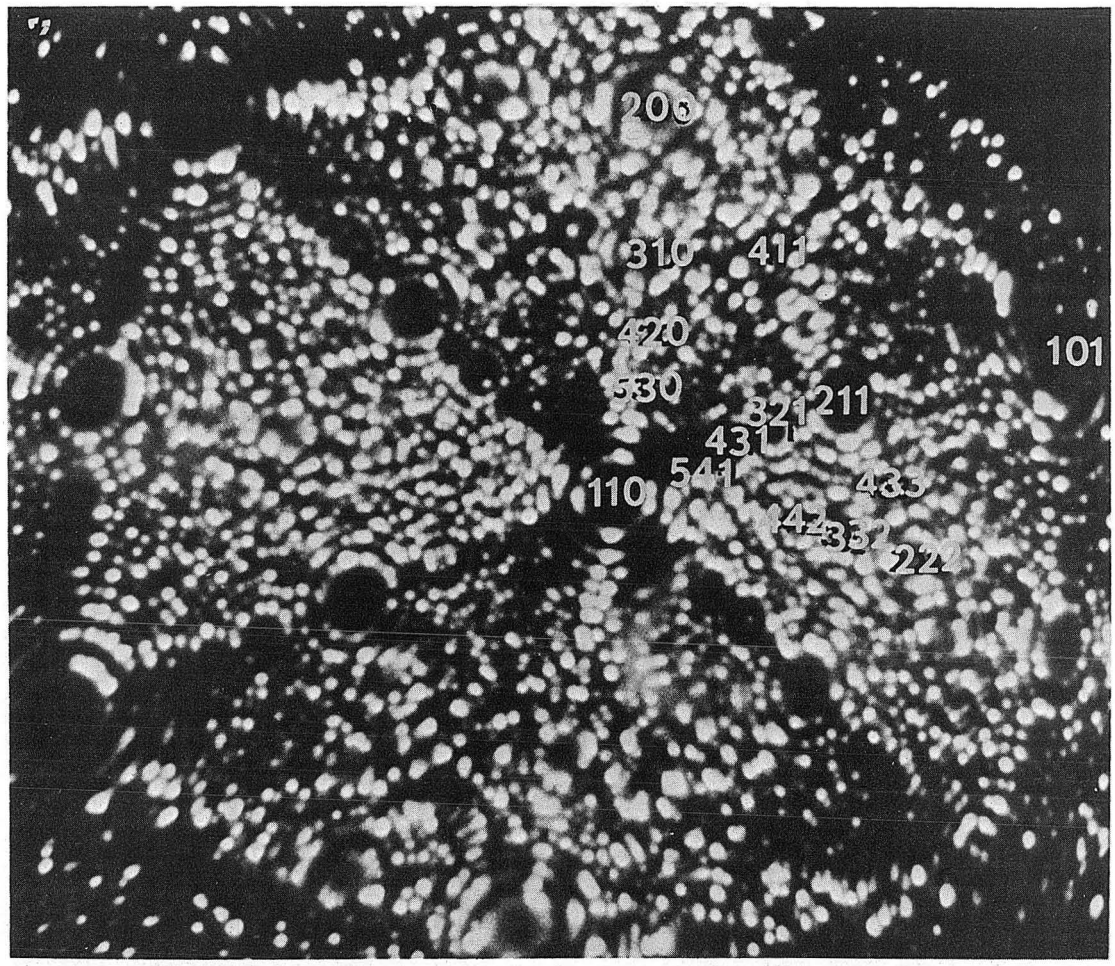

XBB 678-4453

Fig. 2 Helium ion micrograph of Mo at 21°K.

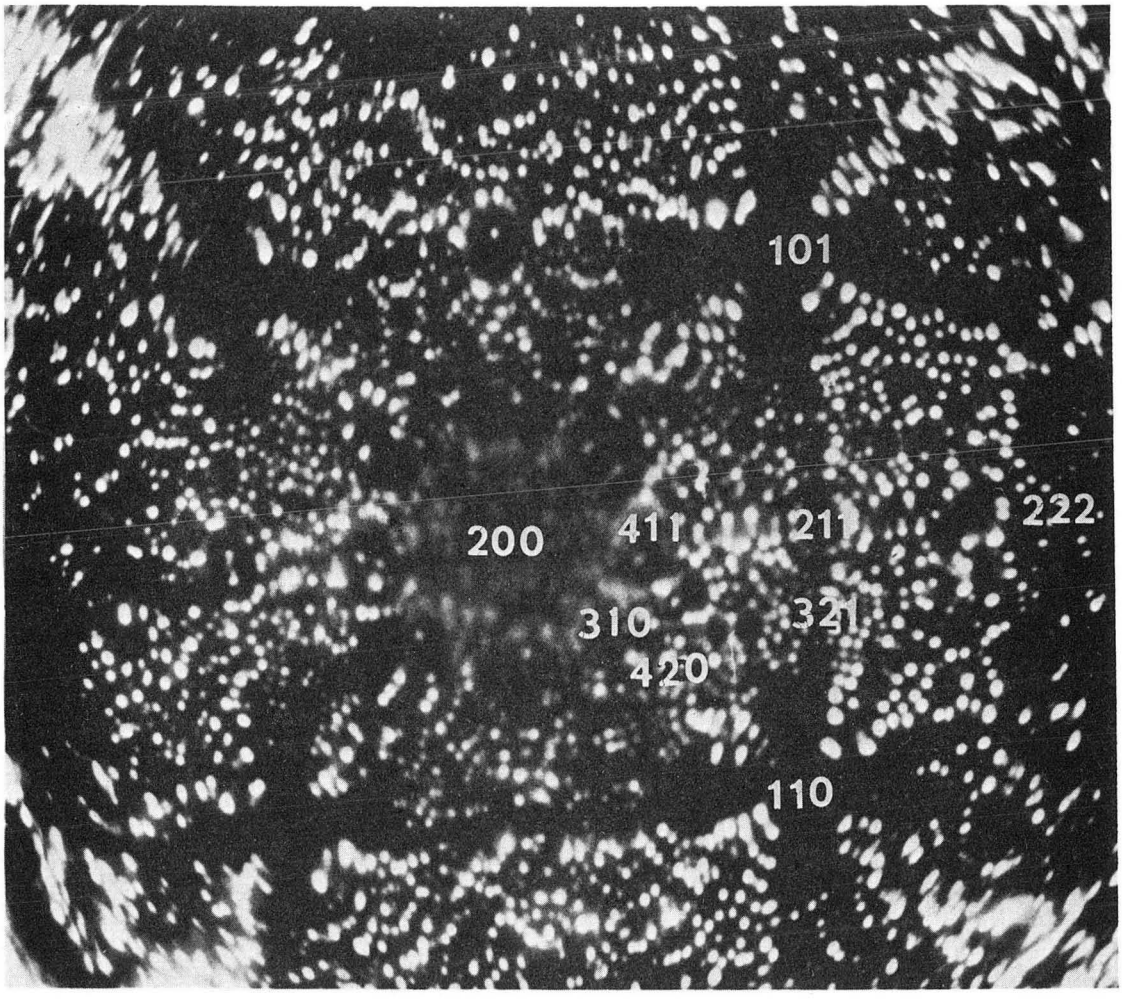

XBB 678-4454

Fig. 3 Helium ion micrograph of Mo-8 Ta at 21°K.

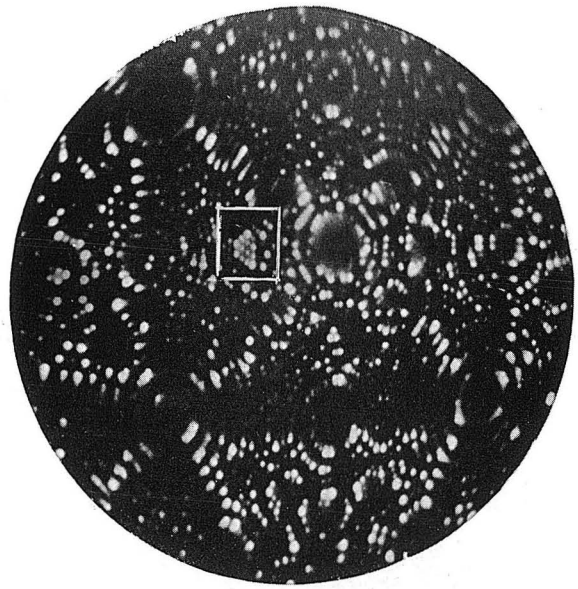

(a)

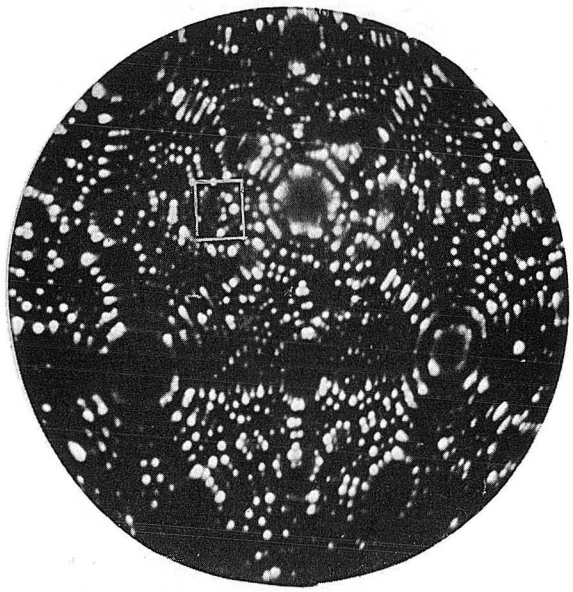

(b) XBB 678-4450

Fig. 4a, b Pulsed field evaporation sequence showing the evaporation of a group of atoms tentatively identified as Ta. (b) was obtained by a single pulse of height 1 kV and duration 30 μsec.

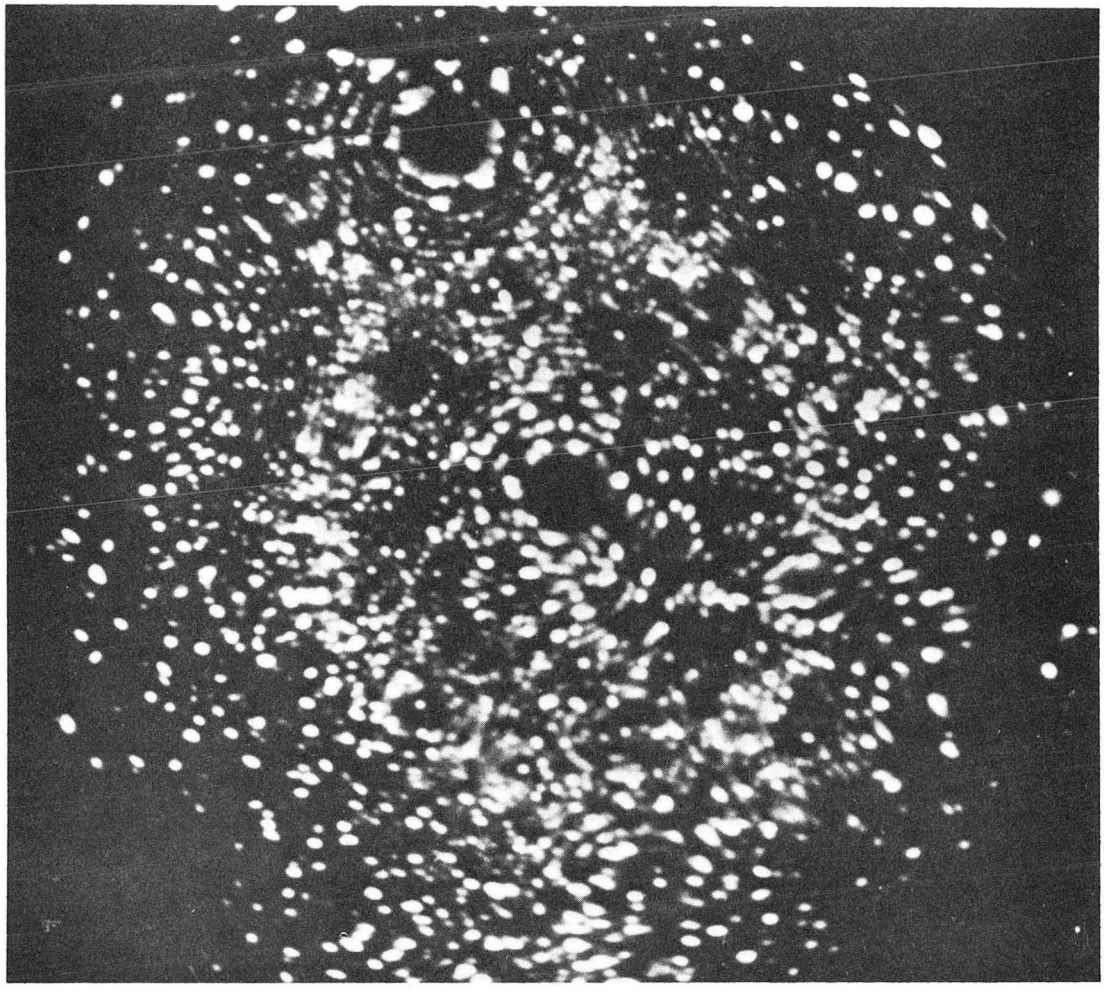

XBB 678-4458

Fig. 5 Helium ion micrograph of Ta-10 Mo at 21°K.

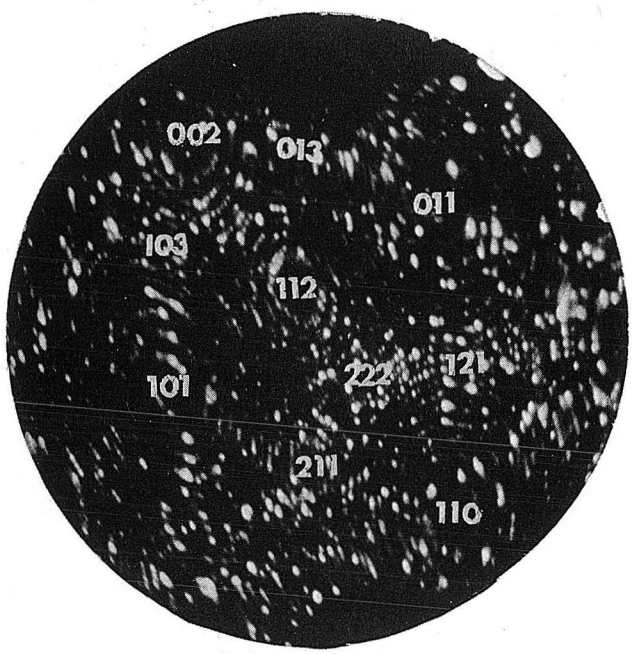

XBB 678-4457

Fig. 6 Helium ion micrograph of Ta-10 Mo showing the presence of dark regions and bright spots.

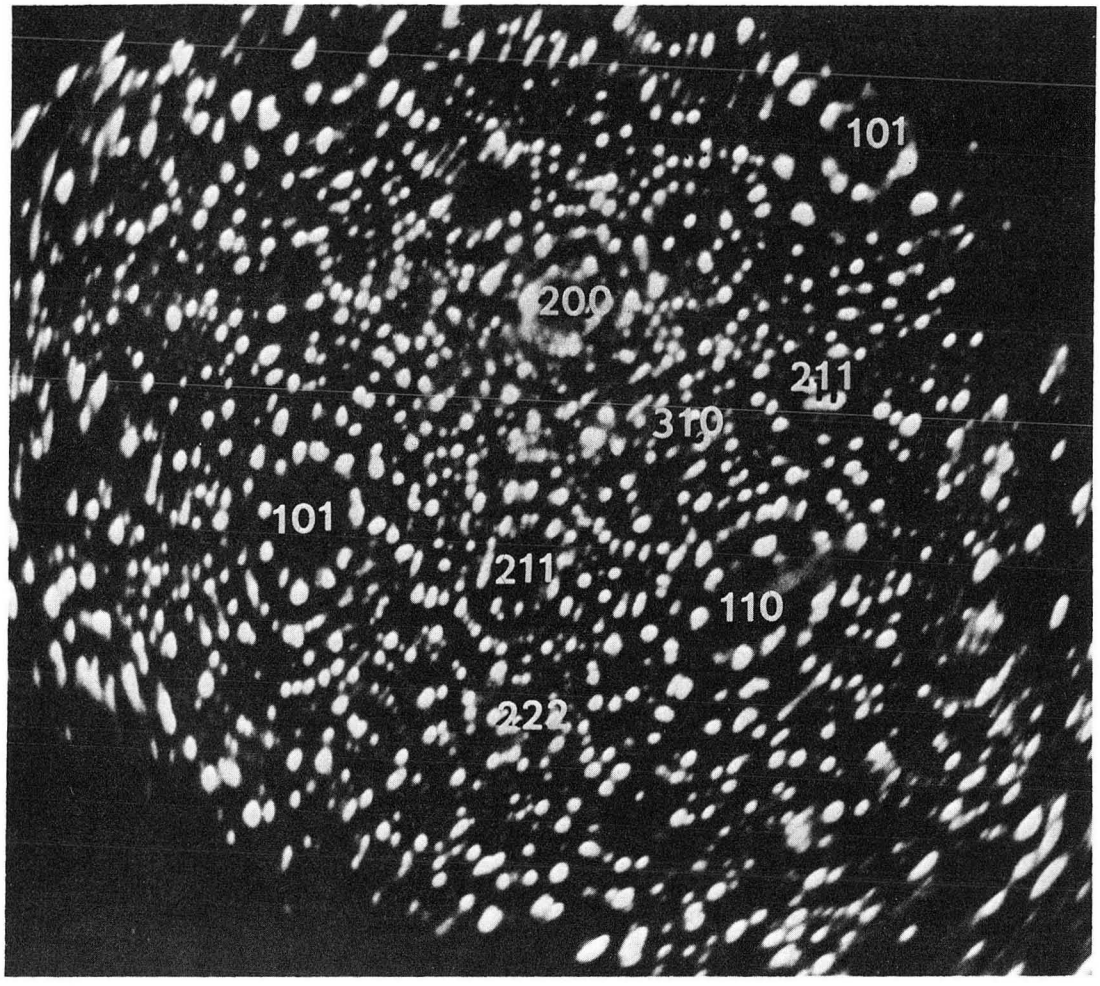

XBB 678-4459

Fig. 7 Helium ion image of Ta-50 Mo at 21°K.

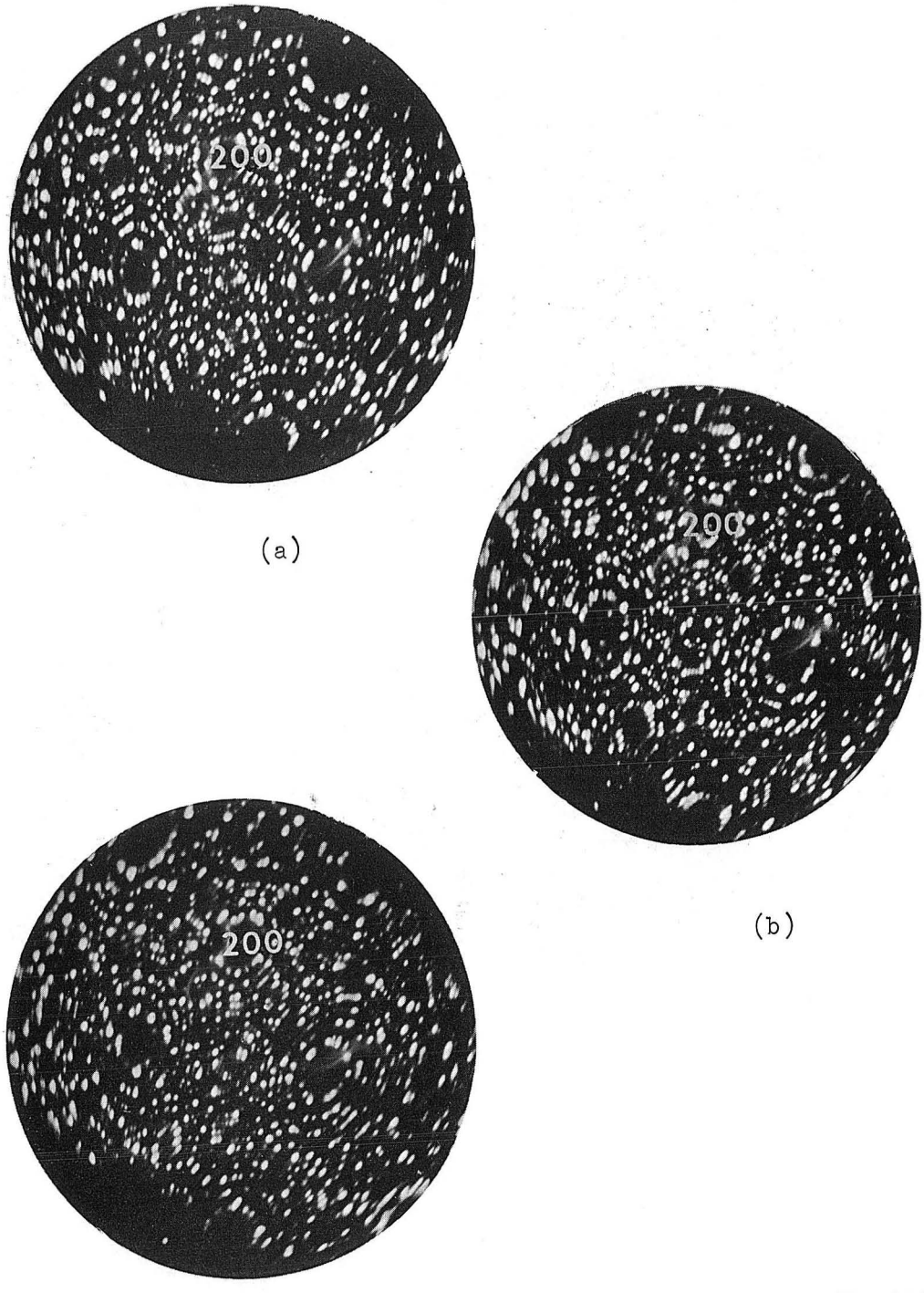

Fig. 8a,b,c Ta-50 Mo micrographs showing a tendency for clustering in the (200) region

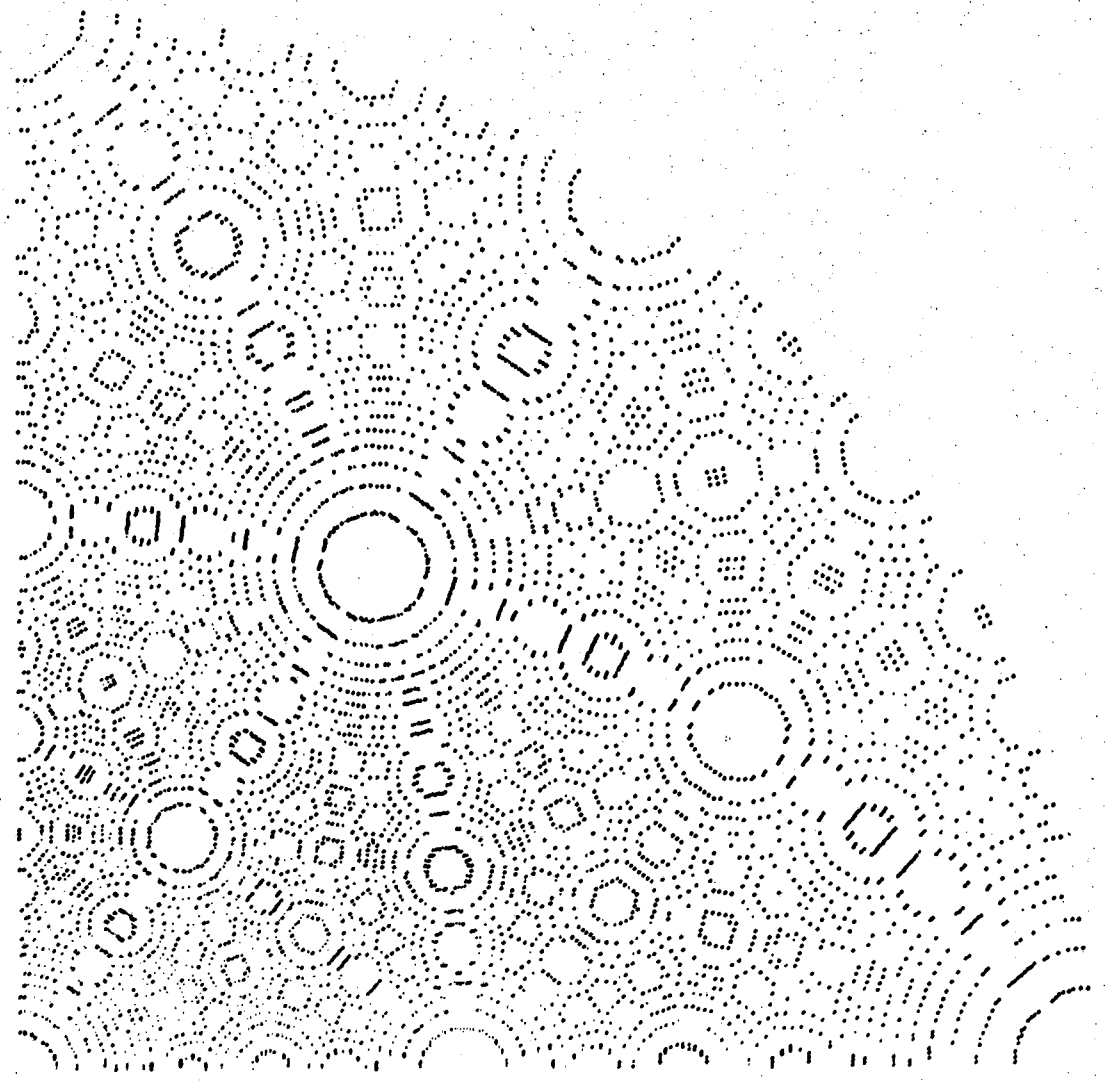

XBL 676-4132

Fig. 9a Computed pattern for a BCC crystal in the [110] orientation. Radius = 200a. Shell thickness = 0.05a.

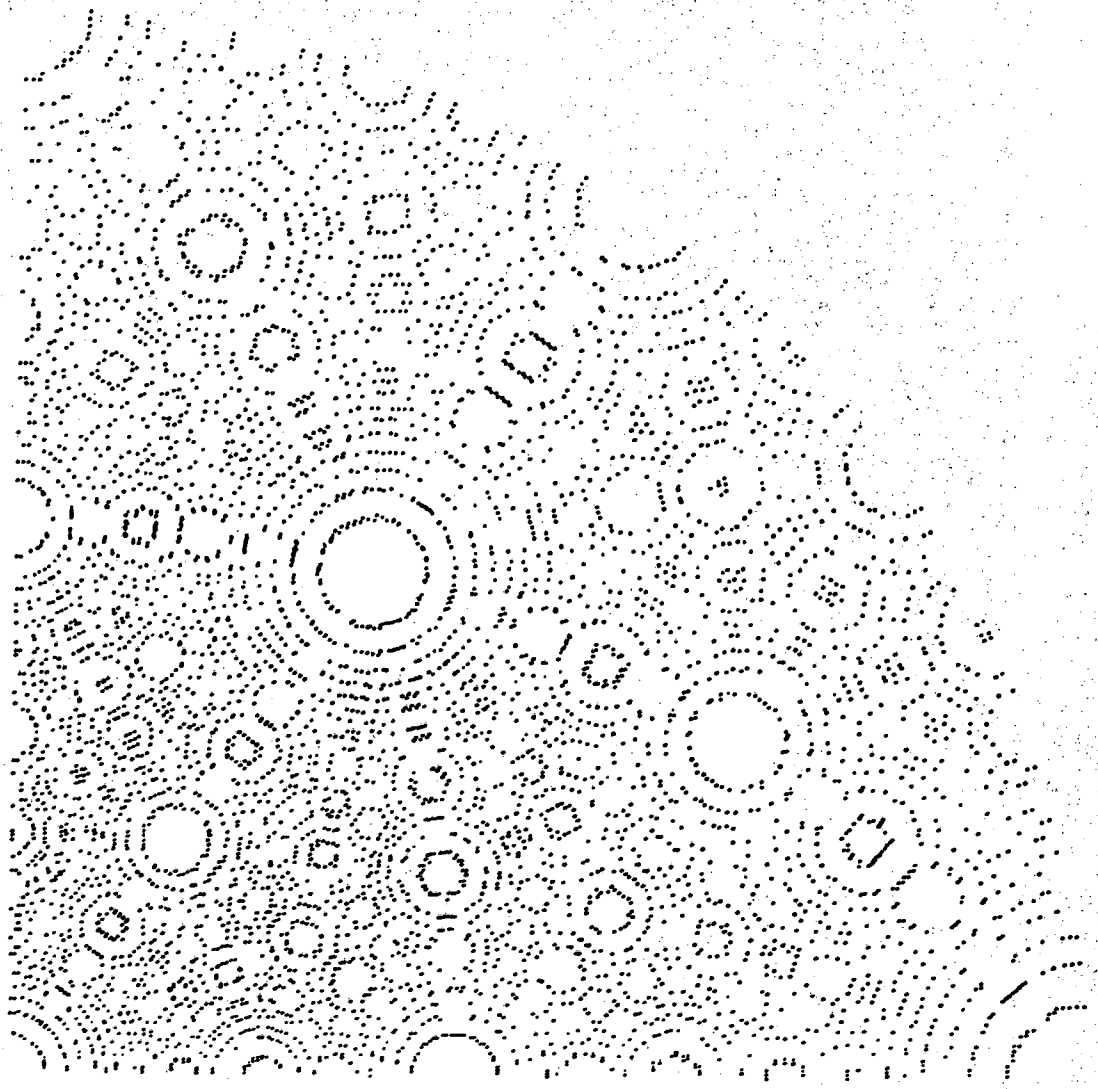

XBL 676-4133

Fig. 9b Computed pattern with total invisibility of solute atoms from alloy of 90% solvent content.

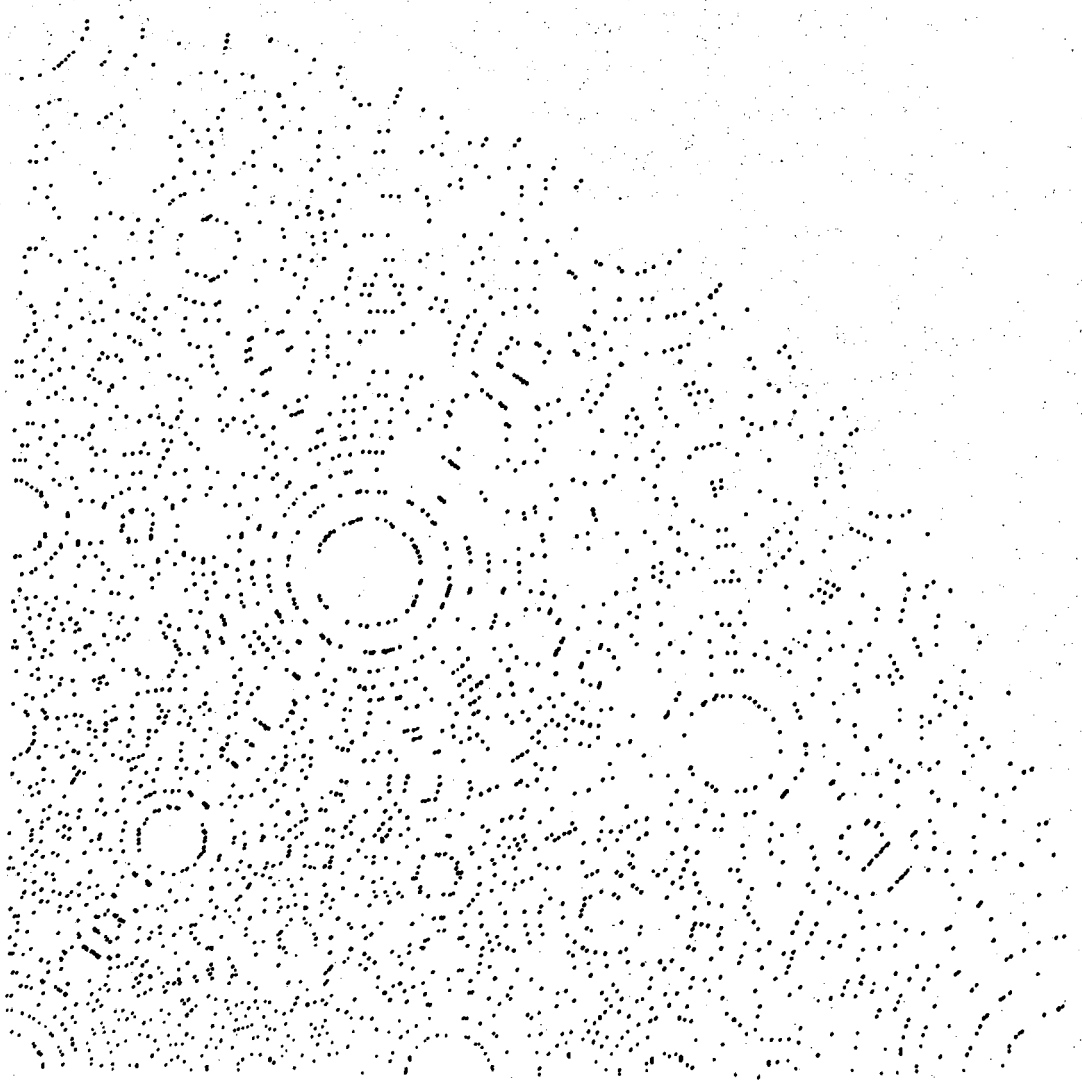

XBL 676-4137

Fig. 9c Computed pattern with total invisibility of solute atoms from alloy of 50% solvent content.

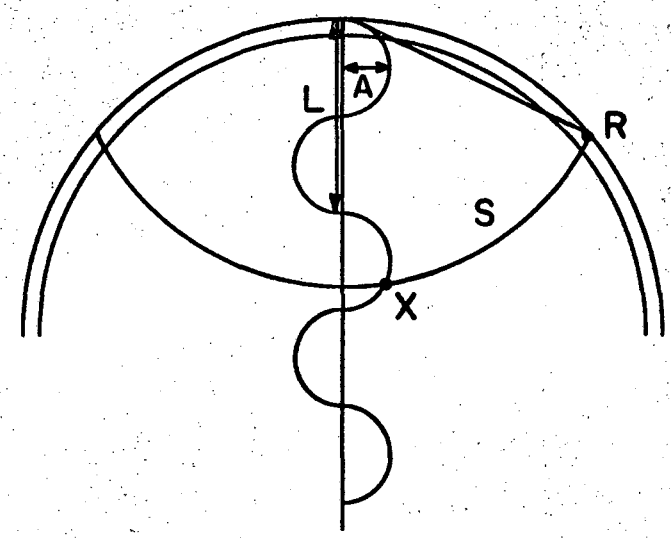

Fig. 9d Cluster geometry for computation.

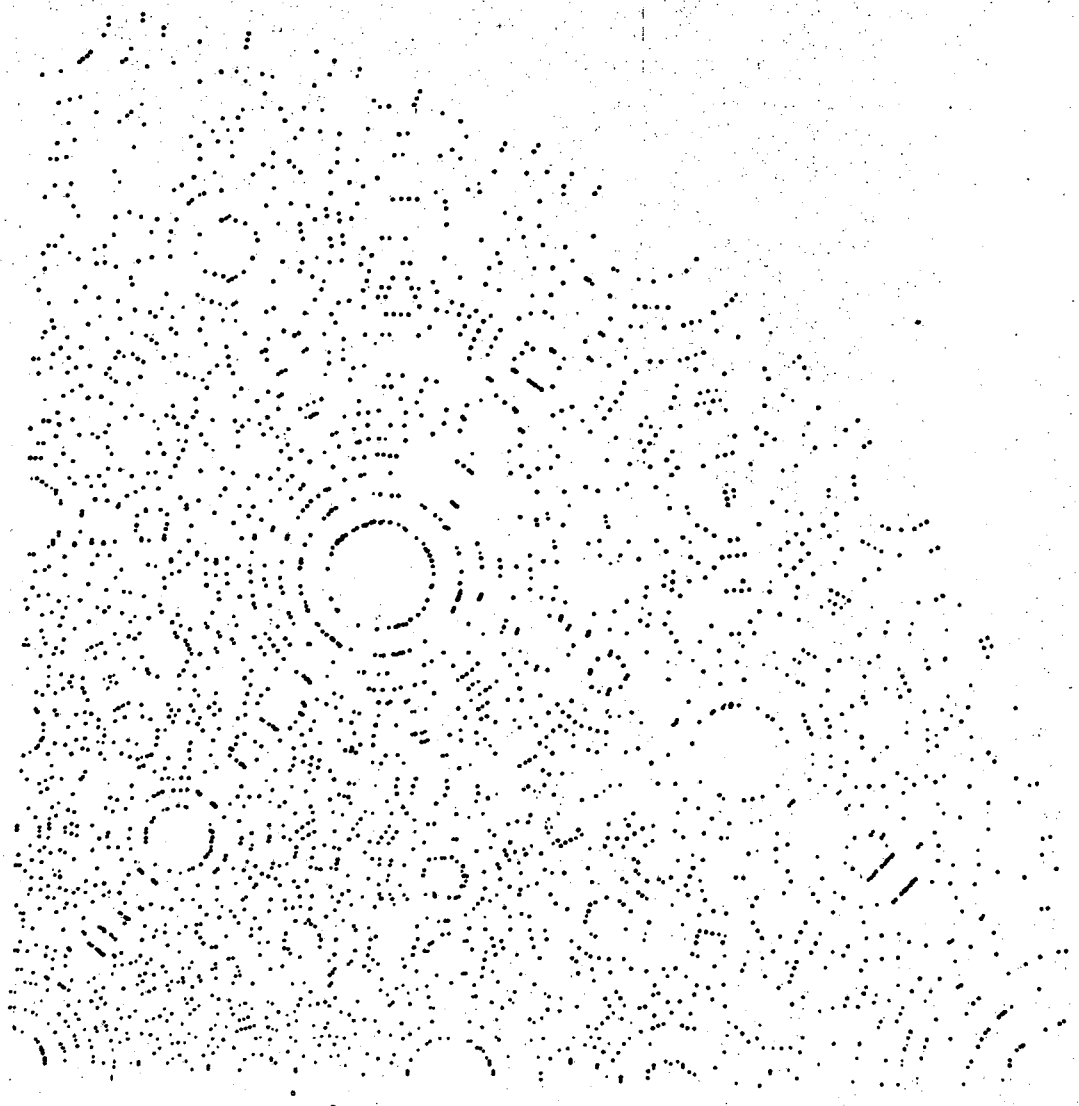

XBL 676-4138

Fig. 9e Computed pattern for clustered alloys. Average composition 50% solvent; cluster period 15 a/$\sqrt{2}$Å and amplitude 0.1.

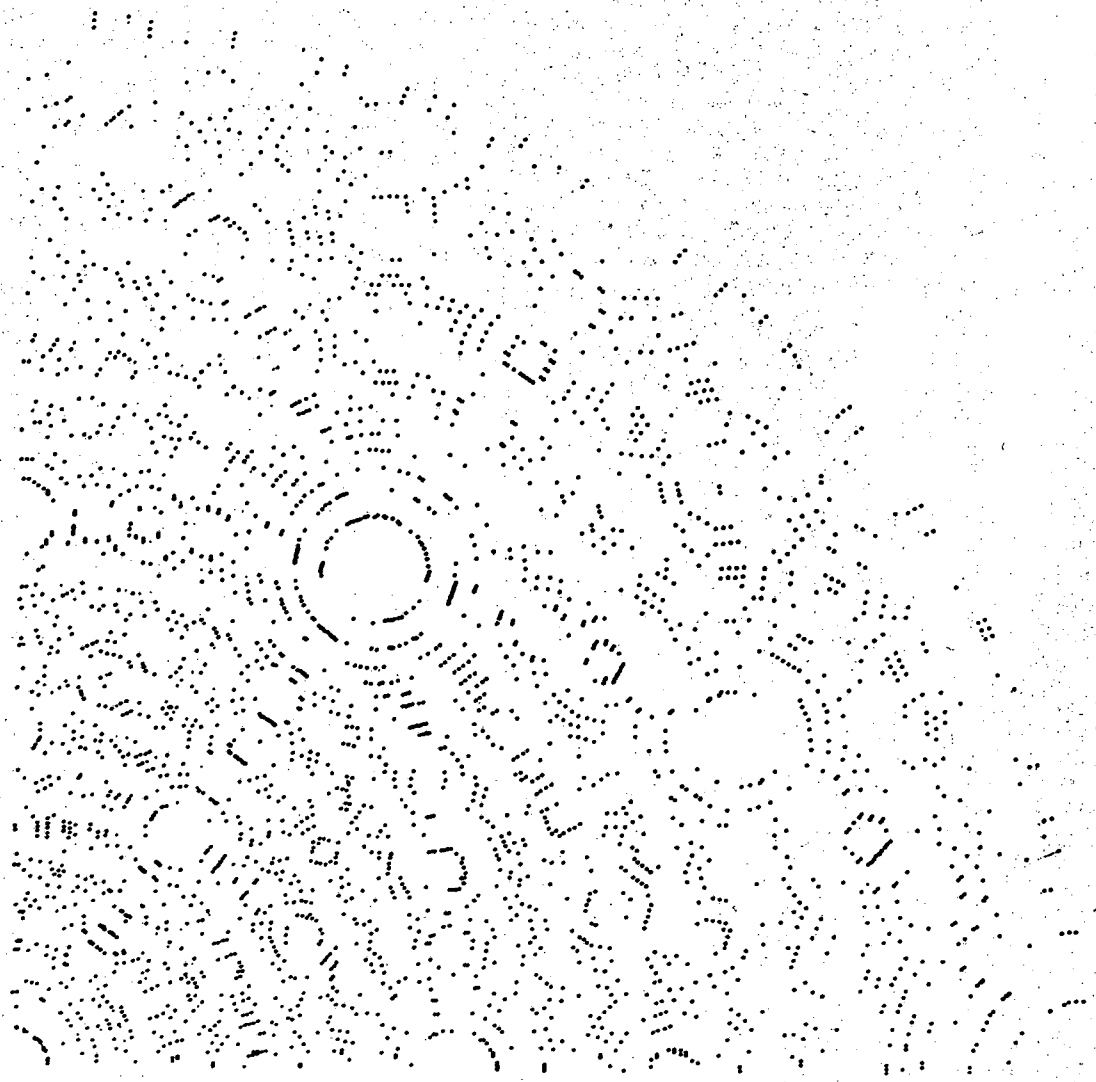

XBL 676-4141

Fig. 9f Computed pattern for clustered alloys. Average composition 50% solvent; cluster period 15 $a/\sqrt{2}$Å and amplitude 0.4.